The Thesis Committee for John Henry Ross
Certifies that this is the approved version of the following Thesis:

An Evaluation of the Self-Healing Capabilities of Fly Ash-based Geopolymers

APPROVED BY
SUPERVISING COMMITTEE:

Maria G. Juenger, Supervisor

Eric van Oort, Co-Supervisor

An Evaluation of the Self-Healing Capabilities of Fly Ash-based Geopolymers

by

John Henry Ross

Thesis

Presented to the Faculty of the Graduate School of

The University of Texas at Austin

in Partial Fulfillment

of the Requirements

for the Degree of

Master of Science in Engineering

The University of Texas at Austin

December 2020

Dedication

To my parents, Michael and Julie, who gave me life, love, and the encouragement that I could do anything I put my mind to.

Acknowledgements

I would like to acknowledge the CODA sponsors and extend my gratitude to our consortium director, Dr. Eric van Oort, for the opportunity to research geopolymers as alternative well cementing materials. Your guidance and drilling industry knowledge proved invaluable to our success as a group.

Thank you to my advisor and CODA co-director Dr. Maria Juenger, for the opportunity to come to the University of Texas at Austin and join the small community of civil engineering materials researchers. Your experimental guidance and love for all things research is an inspiration. Thank you for responding to my emails on weekends and for your investment in my research.

This thesis would not be possible without the countless hours spent by Cameron Horan and Moneeb Genedy in the zonal isolation lab, troubleshooting equipment and executing testing necessary to characterize the performance of geopolymers in the context of well cementing.

Thank you Tesse Smitherman, Daryl Nygaard, Glen Baum, and Gary Miscoe for all the administrative processes crucial to the success of our lab.

Lastly, a special thank you to Virginia Brannaman, as this thesis would not be possible without your love and support.

Abstract

An Evaluation of the Self-Healing Capabilities of Fly Ash-based Geopolymers

John Henry Ross, M.S.E.

The University of Texas at Austin, 2020

Supervisors: Maria Juenger, Eric van Oort

From a drilling perspective, forces in the downhole environment of the wellbore such as tectonic, thermal, and operationally induced stresses can often cause damage to the cement sheath, leading to a loss of zonal isolation due to small fractures that form in the cement sheath along the length of the well. A self-healing cementing material offers the ability to close small microcracks that inevitably form due to the aforementioned stresses in the wellbore, thereby maintaining hydraulic isolation and preventing continued crack propagation with associated gas migration to surface.

One such material previously shown to self-heal is a geopolymer. Geopolymers are alkali-activated cementing materials that have been demonstrated to achieve autogenous self-healing through compressive strength regain. Geopolymers are made from aluminosilicate precursors, such as fly ash, and a hydroxide activator and are cured at elevated temperatures. They can be used as alternatives to traditional portland cement.

The goal of this work was to confirm autogenous self-healing of a Class F fly ash-based geopolymer material and evaluate the extent of self-healing. Self-healing was evaluated through unconfined strength regain and permeability recovery using unconfined

compression and pressure-transmission testing. Samples were stressed after an initial period of curing and then allowed to heal, before being retested for a final time to determine the extent of self-healing.

Initial tests used compressive loading to pre-load the samples to 30, 50, and 70% of their compressive strength at 7 days. Samples were allowed to heal for 21 days before being re-tested to failure. Results unfortunately showed too high of an uncertainty to draw any conclusion about the occurrence of autogenous self-healing. A thermal shock procedure was then developed using liquid nitrogen as an alternative way of micro-cracking the samples. Micro-computed tomography confirmed that the procedure caused micro-cracking in a 25 mm (1 in.) diameter core sample. A baseline pressure transmission test for geopolymers showed that the average permeability of 28-day old specimens was 0.26μD. Pressure transmission testing was then used in a study of self-healing of geopolymers. Results showed that after an initial permeability increase caused by thermal shock damage at 7 days, permeability values for three different samples decreased after a healing period, suggesting that self-healing had indeed occurred. It is the first time such permeability re-healing has been observed and quantified using an appropriate experimental technique.

The results of this study are particularly important in the quest for permanent well abandonment and decommissioning solutions that can be relied upon for long periods of time (e.g. hundreds of years and longer).

Table of Contents

List of Tables

List of Figures

Chapter 1: Introduction

1.1 Motivation

Alkali-activated materials (AAMs), or geopolymers, are a viable alternative to cementitious materials in a wellbore environment due to their comparable compressive strengths and high bond strength in comparison to ordinary portland cement (OPC) [1]. Traditional OPC slurries are prone to contamination by drilling fluids [1], high shrinkage [2], and poor self-healing properties [3]. Specifically, these characteristics of OPC slurries have contributed to failures of abandoned wells due to poor zonal isolation, causing hydrocarbon leakage and blowouts such as at Aliso Canyon [4]. OPC in current wells can become compromised directly after primary cementing due to factors such as autogenous shrinkage [5], thermal loads during production, or geomechanical loads over the course of the lifetime of the well [1].

A material that autogenously self-heals offers the ability to maintain zonal isolation for the well by healing microcracks that would otherwise allow for gas migration in annular spaces behind casing strings and well abandonment plugs in decommissioned wells. Healing of cracks also benefits a wide variety of other structures such as buildings or bridges, where the environmental impact and life cycle costs associated with maintenance of construction materials could be significantly decreased by using a material that spontaneously self-heals [6].

Geopolymers are produced by mixing alkaline activators such as alkali metal hydroxides or silicates with aluminosilicate source materials such as fly ash, ground blast-furnace slag, silica fume, or metakaolin [7]. The result is a complex network of amorphous aluminosilicate reaction products [8], [9]. The high strength and density of the formed

network results in low matrix permeability and high early and final strength [10]. Specific properties such as early strength, workability, and final strength can be optimized for applications, by e.g. adjusting the water-to-solids ratio, varying the alkaline activator, or varying the aluminosilicate source material [8].

Previous work by the consortium on Well Construction Decommissioning and Abandonment (CODA) included research into the effects of non-aqueous fluids such as oil-based and synthetic based muds (OBM/SBM) on geopolymer strength by contaminating mixtures with varied amounts of OBM/SBM. Under triaxial loading, both the OBM/SBM-contaminated geopolymer hybrids and neat geopolymers exhibited more ductile failure behavior than OPC [3], [11]. Moreover, the neat geopolymers and contaminated mixtures also showed autogenous self-healing strength regain under 3.45MPa (500 psi) confining stress for multiple samples initially loaded at 7 days and re-tested to failure at 28 days. The peak stresses of two geopolymer samples increased by over 30%, whereas the OPC mixtures showed a significant decrease in peak stress [3].

1.2 OBJECTIVE

This goal of the work presented in this thesis was to further investigate the autogenous self-healing properties first shown by Liu and Liu et al. [3], [11], by first confirming prior unconfined strength self-healing results and then expanding testing to determine the extents of self-healing. The research questions for this work were as follows:

1. Is the autogenous self-healing behavior shown by Liu and Liu et al. [3], [11] repeatable?
2. Is unconfined compressive strength testing accurate enough to provide evidence of self-healing?

3. Is thermal shock an effective method to create micro-cracking for self-healing experiments?
4. What is the range of gas and fluid permeability for geopolymers? Is it comparable to a typical portland cement slurry?
5. Do geopolymers show self-healing through permeability testing?

1.3 THESIS ORGANIZATION

This thesis is organized into four sections. Chapter 2 provides a literature review detailing a background of geopolymers, motivation for self-healing materials, and studies detailing relevant techniques to test for self-healing. Chapter 3 introduces a description of materials used and detailed experimental methods. Chapter 4 presents the results of self-healing testing and a discussion of the effectiveness of different techniques used. Lastly, Chapter 5 summarizes the results on autogenous self-healing of geopolymers and suggests ideas for future work.

Chapter 2: Background

2.1 GEOPOLYMERS

Alkali-activated materials have been known as an alternative to portland cement since 1908, and their use has been documented throughout the world over the course of decades since discovery [8]. Fundamental microstructural characterization of AAMs started in earnest in the 1990s, and recent work has begun to focus on overall performance as these materials are transitioned into use. New areas of research include service life, mechanical performance, and durability [8].

Geopolymers are a subset of AAMs, with low calcium contents. The term was first coined in the 1970s by Davidovits, naming the material for its origins in geological materials [8], [9], [12]. Geopolymers are formed from the reaction between an aluminosilicate source material and an alkaline solution. Similar to cement hydration, the activation of geopolymers involves the combination of a dry binder and a fluid activator. The process of geopolymerization is not fully understood, but researchers agree there is dissolution of the solid binder and condensation of gel products that harden to produce the final structure [3], [8], [12]. The aluminosilicate network structures are sometimes referred to as N-A-S-H or C-(A)-S-H gels, where N represents sodium oxide, A is alumina, S is silica, C is calcium oxide, and H is water [13]. Depending on the activator and aluminosilicate source materials, geopolymer gel composition varies [8]. One option for a dry binder is fly ash, a coal combustion waste product. Previous geopolymer research found that if all other experimental variables are held constant, the ratio of alkaline activator to fly ash greatly affects the rate of geopolymerization [14]. Along with other sources of variation such as activator solution and fly ash type, geopolymers have a wide variety of possible mixtures that can be subsequently altered to affect performance.

2.2 SELF-HEALING MATERIALS

Self-healing behavior in the context of cementitious materials is defined as the ability of a material to repair microstructural cracking without any external intervention [15], [16]. This can be subsequently broken down into two subcategories of autogenous and autonomous self-healing. In autogenous self-healing there are no alterations to the material properties, whereas in autonomous self-healing there are embedded systems to cause self-healing upon damage to the microstructure [17]. The two main mechanisms of autonomous self-healing include either bacteria or embedded capsules that react upon damage to the microstructure [17]. The work reported in this thesis only examined autogenous self-healing.

Self-healing of portland cement materials has been widely observed throughout the world and is often attributed as the reason why centuries old structures are still standing today. In the early nineteenth century, self-healing was recorded in pipes, culverts, and retaining structures [18]. This is also well-recorded for AAMs, where one example widely referenced is an irrigation pipeline comprised of ground blast-furnace slag concrete. Its early strength of 25MPa increased to over 80MPa when tested around 30 years later after extensive use [18]. The ability of materials to self-heal is now well-established, but new technology has allowed for specific properties conducive to self-healing to be enhanced or improved [16].

Much of the available self-healing literature focuses on the self-healing of concrete or geopolymers in a civil engineering context. This literature review assumed much of the knowledge of self-healing is transferrable between civil engineering and drilling applications.

2.3 Climate Change: The Role of Geopolymers and Self-Healing

As anthropogenic climate change continues to define policy efforts throughout the world, carbon emissions associated with the built environment will continue to come under scrutiny. Efforts are now being focused on ways to reduce demand and increase the service life of structures and cementing applications. The main ideas at the forefront of decreasing the carbon footprint of the built environment include increasing the durability of new construction through self-healing materials and developing alternative binders that are less carbon intensive [16], [19].

One measure towards improved sustainability has been the use of AAMs as low-carbon alternative cements [20]. The environmental impact of the aluminosilicate source materials is quite low, considering many of the sources are waste by-products of coal combustion or metal production. Governments are now facing pressure to avoid the landfilling of these high-volume products [8]. Most of the carbon footprint of AAMs comes from the production of the alkali and silicate activators. A recent study on the environmental impact of geopolymers found that some geopolymer cements could reduce the global carbon emissions associated with concrete production by a factor of 4, depending on the activator [20]. Other experts estimate the potential carbon dioxide savings are on the order of 80% in comparison with portland cement on a binder-to-binder basis [8]. This makes AAMs quite advantageous in reducing the carbon footprint on a given project in comparison to traditional portland cement.

Another measure towards increased sustainability has been to increase the durability of binders used in structures, thus expanding service life, and reducing the need for new construction. Cracking in concrete is almost unavoidable, due to its brittle behavior under loading, the harsh environmental conditions to which it is often subjected, and

irreversible shrinkage due to drying [15], [16], [21], [22]. Cracks allow for harmful substances to enter, compromising durability due to an increased rate of corrosion of reinforcement or degradation of the cementitious matrix [15], [23]. Cracking also compromises the performance of the mechanical properties of the concrete. Thus, a self-healing concrete is highly desired to regain properties lost due to damage and increase the lifetime of concrete structures [16], [23], [24]. From a life-cycle modeling perspective, it has been shown that the initial investment into higher quality materials during construction ultimately outperforms using lower quality materials due to repair costs over time [16]. Several positive implications for self-healing structures include the reduced need for: raw materials, energy, and rebuilt construction [16]. Illustrating this effect, Figure 2.1 shows that typical structures undergo repairs over time that often are associated with increased costs of maintenance as reliability decreases. The structure made from the self-healing material can continually repair itself, maintaining its performance above required strength and a constant cost.

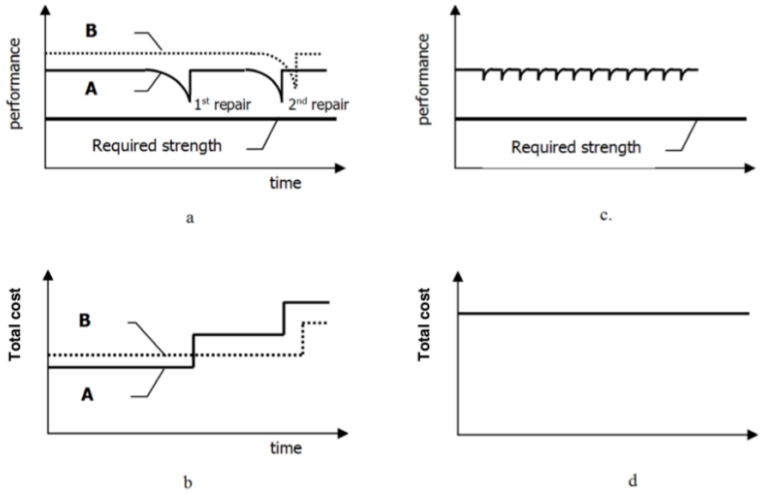

Figure 2.1: Performance and cost over time graphs for (a,b) a normal structure and (c,d) a structure made with a self-healing material. Reprinted with permission from [6].

2.4 Techniques to Measure and Detect Self-Healing

2.4.1 Macroscale Techniques

Unconfined compressive strength (UCS) measurement is a simple and cost-effective way to identify the extent of self-healing, because it can be used to probe for strength regain after initial loading [3], [11]. As samples undergo loading in compression, stresses in the material cause internal damage and cracking up until failure. Loading samples to a strain that approaches failure causes cracks to form in the material, which can then be healed during the self-healing period. After the self-healing period, samples are retested to failure and peak stress values are compared to the ultimate strength of virgin samples of the same age [3]. For the material to be truly beneficial as a self-healing material, it should have at minimum the same strength as the virgin samples that did not

undergo damage. The benefits of using UCS measurement for this purpose include its cost effectiveness and its wide acceptance as the predominant factor in quality of concrete, thus demonstrating that strength regain is paramount in defining extents of self-healing [25]. Often, a major drawback to UCS testing is that the test is prone to error because of point loading, non-parallel loading surfaces, and inconsistent loading rates. One way to reduce point loading effects is to use neoprene or sulfur caps on cylinders. Grinding samples to have parallel loading surfaces can also result in more consistent results due to a more even compressive load distribution across the loaded surfaces. Confined compression or triaxial compression tests are considered less prone to error because of the confining stress around the sample which prevents lateral movement and allows for a higher strain to be reached before failure. This useful in self-healing tests, where the sample can be damaged to a greater degree before reaching compressive failure.

Another method to determine the extent of self-healing on a macroscale level is using bending tests to create microcracks. Bending tests are used to establish tensile strength. In the context of self-healing, a maximum crack mouth opening displacement (CMOD) value can be used to limit induced cracks in samples [26]. This limit allows for consistency in the size, orientation, and number of cracks formed, where size greatly affects self-healing extents [17], [22], [26]. Initial loading causes cracks to form in the samples, which result in a reduced stiffness upon loading. Without self-healing occurring, the re-loading of the samples would cause failure at a lower strength due to the reduced stiffness. With self-healing occurring, the tensile strength would increase beyond the initial load that caused cracking, showing that the material has self-healed. Additionally, the material will propagate new cracking upon reloading if cracks heal to an equivalent or greater strength when compared with the virgin material [16]. This behavior is illustrated in Figure 2.2.

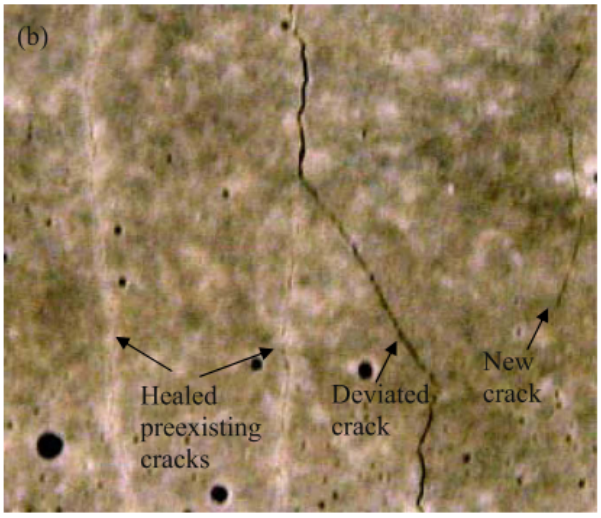

Figure 2.2: Optical microscopy image showing new crack propagation after self-healing and retest. Reprinted with permission from [27].

One last method of macroscale testing to determine self-healing tendency is permeability measurement. Permeability is the ease by which a fluid or a gas passes through a porous material, and can be tested using a variety of methods [28]–[31]. Gas and fluid permeabilities differ and vary based on the gas or fluid used for testing. Cracks generally interconnect pores in the microstructure of materials and allow for fluids or gas to migrate faster through the structure, reflected by an increase in the permeability of the material [31]. After induced cracking using one or more methods, permeability will increase. Moreover, after self-healing, permeability should decrease due to the presence of healing reaction products. Using permeability to measure self-healing was utilized in the very first investigations into self-healing in concrete [29]. In this case, flow rate (in L/hr.) was used to denote the permeability of the concrete containing large cracks, and the change in water flow rate after a certain period of self-healing was measured. Most researchers in

the present-day opt for similar low cost, low pressure permeability tests that take days to reach steady-state flow, but they yield good results [30], [31]. For geopolymers, no permeability data are currently reported in the literature. Typical portland cement water permeability values for Class H and G cement slurries are reported from under 1 μD to well into the millidarcy range [32]–[34]. Note that in the context of well cementing, the American Petroleum Institute recommends that well cement permeability not exceed a value of 10^{-16} m^2 (100μD) [35]. With very low permeabilities, it becomes increasingly difficult to determine permeability using flow rate tests, and more sensitive pressure tests (such as the pressure transmission test discussed below) are necessary.

An important point with permeability testing is that it reflects on a material's ability to regain hydraulic isolation, which is essential to zonal isolation in oil and gas wells. Note that it is actually insufficient for a well cementation material to regain strength if it not also regains its ability to regain the hydraulic isolation characteristics of a properly functioning barrier to annular fluid and gas migration.

2.4.2 Microscale Techniques

Optical microscopy is an inexpensive and popular way to visualize crack closure due to self-healing. As previously shown in Figure 2.2, the healed cracks can be clearly observed and differentiated from the deviated and new cracks by the colors and contrast in the optical microscopy image [27]. New crack propagation, seen in the black lines in Figure 2.2, is the best indicator for a self-healed material, meaning that the healed pre-existing cracks are stronger than the uncracked planes. Deviated cracks can also occur as a part of new crack propagation, where the dark crack lines meet the white lines of self-healing reaction products, illustrating areas where the self-healed cracks are weaker than the

uncracked planes. Overall, optical microscopy is an effective tool in determining failure modes during self-healing testing, but other techniques offer further in-depth analysis of self-healing products.

Energy dispersive x-ray spectroscopy (EDXS) has been used to analyze the composition of the healing products formed in microcracks [27]. In this case, the study focused on Engineered Cementitious Composites (ECC), a cementitious material that uses fibers to create additional ductility. Samples that had healed were imaged using scanning electron microscopy (SEM) and EDXS analysis. The result, shown in Figure 2.3, demonstrated that the main composition of the healing product was calcium carbonate. This technique allows researchers to confirm what self-healing processes are occurring by assessing microstructural composition.

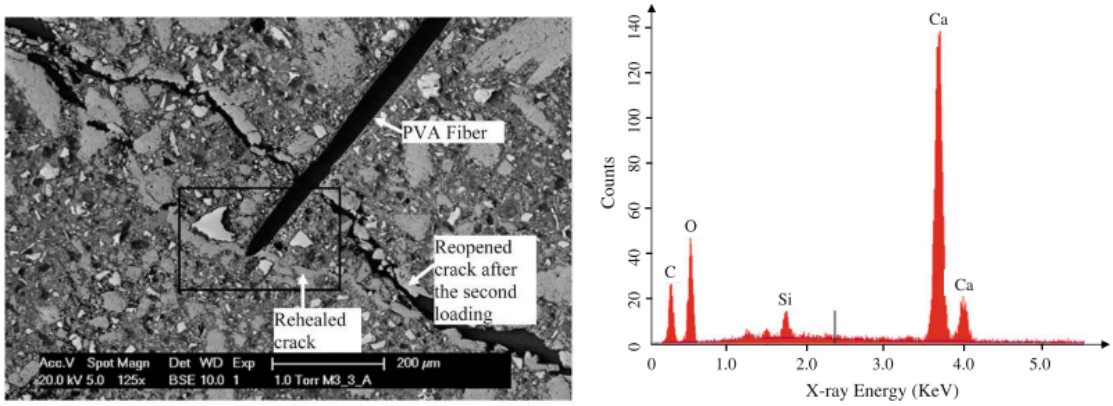

Figure 2.3: SEM (left) and EDXS (right) for ECC after self-healing and retest. Reprinted with permission from [27].

In a recent study of self-healing properties of ECC, researchers utilized x-ray computer microtomography (µCT) to image 3-D micro-cracking [22]. Point clouds were obtained from the 3-D scans and subsequently reconstructed to calculate a volumetric

difference in self-healing before and after micro-cracking. In addition, SEM and EDXS were used to analyze the composition of the healing reaction products formed in the microcracks of the ECC subjected to micro-cracking and cycled wet/dry cycles to produce self-healing. The SEM and EDXS revealed that the cycles initiated unreacted cement to hydrate and form C-S-H in the microcracks. Imaging was done at 1, 5, and 10 cycles to see the formation progress. As denoted in Figure 2.4, researchers processed the μCT data to isolate the gas phases within the structure and used further processing techniques to isolate cracking from pores within the composite [22]. This study shows great potential for self-healing research using imaging techniques to quantify self-healing.

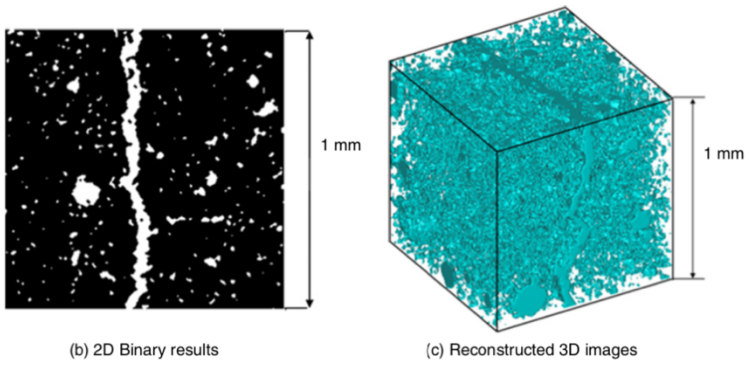

Figure 2.4: μCT data processing for gas phase isolation. Reprinted with permission from [22].

2.5 Autogenous Self-Healing Mechanisms in Cementitious Materials

To understand the mechanisms of autogenous self-healing in cementitious materials, the reaction products of cement hydration must first be defined. The main products formed in the cement hydration reaction are calcium silicate hydrate (C-S-H), calcium hydroxide (CH), and ettringite. Both C-S-H and CH are involved in the chemical

processes in autogenous self-healing, but there is no evidence that ettringite is involved. Calcium silicate hydrate is referred to in cement chemistry notation as C-S-H due to the fact it has no fixed stoichiometry and exists in cementitious systems in a variety of forms. C-S-H is a layered material that binds the aggregate and unreacted cement particles together inside a hydrated cement system, and is thereby largely responsible for the strength of the system.

One cause of self-healing may be the swelling of the hydrated cement paste near the crack faces, due to the uptake of water from the crack interface [6], [17]. In this process, water enters through the crack and migrates into the structure of the matrix, causing swelling of the cement paste. It is estimated that this process results in less than 10% reduction of fluid flow through the crack. Thus, its self-healing contribution is considered minimal in comparison with chemical processes [6].

Chemical processes of autogenous self-healing can be subdivided into two types: the continued hydration of unreacted portland cement and the formation of calcium carbonate [6], [17]. The continued hydration mechanism of self-healing is dependent upon an excess of unreacted cement particles. As water enters the crack, unreacted cement reacts with the water and the hydration products fill in the crack. The creation of C-S-H as a continued hydration product can provide the adhesive strength necessary to bridge a crack. The C-S-H also serves as a nucleation site for other self-healing reaction products such as calcium carbonate to grow.

Calcium carbonate forms in cementitious materials at atmospheric conditions through the reaction of atmospheric CO_2 in the pore solution with calcium ions dissolved in the pore solution, as shown in Equation 2.1.

$$Ca^{2+} + CO_2 \rightarrow CaCO_3 + H \qquad (2.1)$$

Calcium ions in solution typically come from CH, which dissolves further as calcium ions are consumed through the reaction with CO_2. The calcium carbonate occupies more space than the calcium hydroxide originally did, explaining how crack closure can occur if there is enough calcium hydroxide and carbon dioxide present. Once CH is exhausted, other calcium-bearing phases can also provide calcium in solution. The reaction rate varies depending on temperature, pH, and concentration of reactants [29]. This mechanism of autogenous self-healing has been considered the most effective by the extensive investigation by Edvardsen [6], [29].

Edvardsen conducted early research into the autogenous self-healing behavior of concrete by subjecting cracked concrete to water pressure and by observing how factors of crack width, materials used in concrete, and water flow affected the ability of concrete to self-heal [29]. Representative results are shown in Figure 2.5. It was found that the growth rate of calcium carbonate crystals was dependent on crack width and water pressure, while the materials used in the concrete had no effect on the healing rate. Additionally, Edvardsen [29] discovered that the initial crystal growth is surface-controlled, whereas after the initial phase of water exposure it becomes diffusion-controlled. The majority of autogenous self-healing was determined to occur during the first 3 to 5 days of exposure, depending on factors such as water pressure and crack width. It was found that the larger the crack width and greater the water pressure, the lower the degree of self-healing [29].

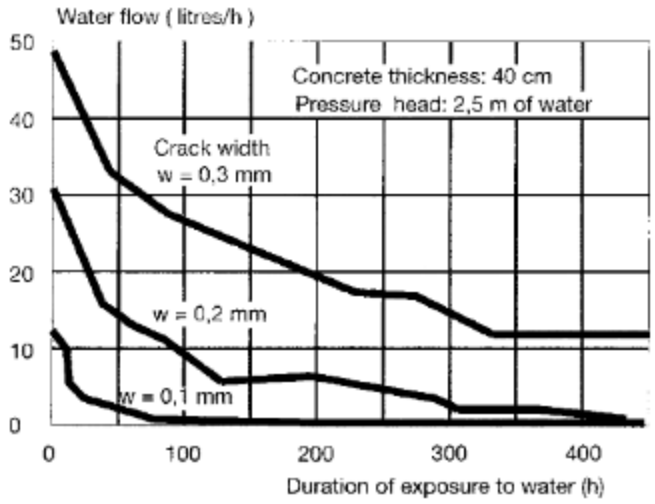

Figure 2.5: Relationship between water flow and time for different crack widths (per m of visible crack length). Reprinted with permission from [29].

Limiting the size of cracking in materials is key in self-healing, and one such way to achieve this is using polymer fibers to create ECC [22]. The fibers, typically added to concrete in 2% vol. or less, aid in dissipating loading energy to create small microcracks in the structure, which can later be self-healed. The fibers also increase the ductility of the concrete, increasing the tensile strain capacity to between 2 and 5 percent, which is hundreds of times greater than that of normal concrete [36]–[38]. The main mechanism of autogenous self-healing observed in this type of system is the precipitation of calcium hydroxide and calcium carbonate due to the presence of moisture in the system [15]. The fibers, while constricting the size of cracking, also serve as nucleation sites for self-healing products to grow. Figure 2.6 shows an optical microscopy image of ECC, where the white calcium carbonate precipitate formed in the microcracks contrasts with the grey hydration products quite clearly.

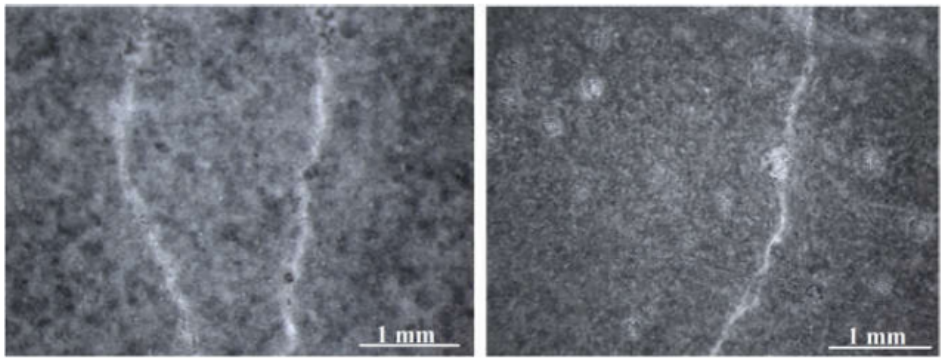

Figure 2.6: Optical microscopy images illustrating formation of calcium hydroxide and calcium carbonate in cementitious composites. Reprinted with permission from [15].

In a different study into the self-healing ability of ECC, self-healing in samples at early ages increased with the number of healing cycles (water/air exposures), but eventually plateaued after approximately 4-5 cycles. The presence of water was determined to be the critical factor in self-healing product formation due to the excess of water and the increased rate of dissolution of CH at the crack surface, causing further hydration [36].

In contrast, an investigation into the effect of exposure on autogenous self-healing in portland cement mortars concluded that the specific self-healing products were dependent on the mixture composition and independent of the applied exposure conditions [39]. The application of varied amounts of water present during curing did not affect the degree of self-healing, suggesting that the higher ion concentration present in samples with lower water volume does not result in greater self-healing. The introduction of micro-silica into the conditioning solution resulted in the greatest amount of self-healing, attributed to the micro-silica serving as nucleation sites for self-healing products such as C-S-H, CH, and $CaCO_3$ [39]. Nucleation sites provide areas for self-healing reaction products to precipitate and grow, allowing for greater degree of self-healing to be reached.

Additionally, admixtures such as a phosphate-based retarder were shown to produce the highest degree of crack closure in mortar samples, with a possible mechanism shown in Figure 2.7. It was postulated that phosphate ions caused the formation of calcium-phosphate healing products and prevented the creation of hydration products around the cement grain, allowing for further hydration of unreacted cement during the self-healing event. Additional work on large scale samples and x-ray powder diffraction (XRD) would confirm results and phases that were assumed to be present.

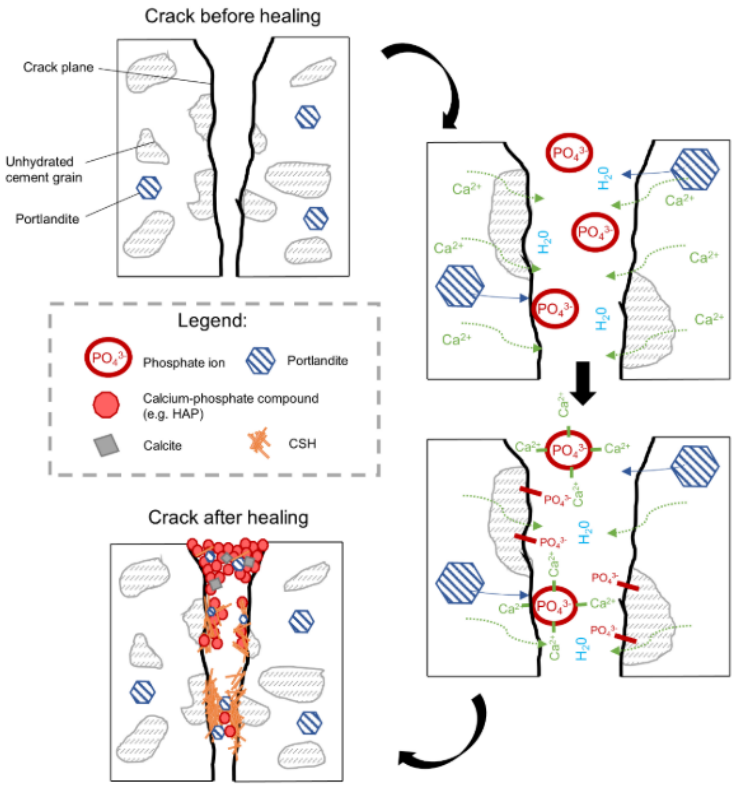

Figure 2.7: A possible mechanism for self-healing using a phosphate-based retarding admixture. Reprinted with permission from [39].

2.6 AUTOGENOUS SELF-HEALING IN ALKALI-ACTIVATED MATERIALS

In the case of AAMs, continued reaction is the dominant mechanism thought to be contributing to self-healing behavior observed, since not all alkali-activated systems contain enough calcium to form the dominant phases responsible for self-healing in concrete such as C-S-H and $CaCO_3$ [11], [18]. Results from Liu et al. [11], shown in Figure 2.8, illustrated autogenous self-healing strength regain in low calcium fly ash geopolymer pastes of over 30% of the initial loading under confined compression testing [3], [11]. In unconfined compression testing, results showed a similar regain in strength above initial failure values. The geopolymer pastes outperformed the portland cement pastes in percentage of compressive strength regain, an indication of greater self-healing ability. This denotes a possible advantage in using geopolymer cements in both building and well construction applications in comparison to portland cement, as strength is the key performance metric needed from a structural engineering standpoint.

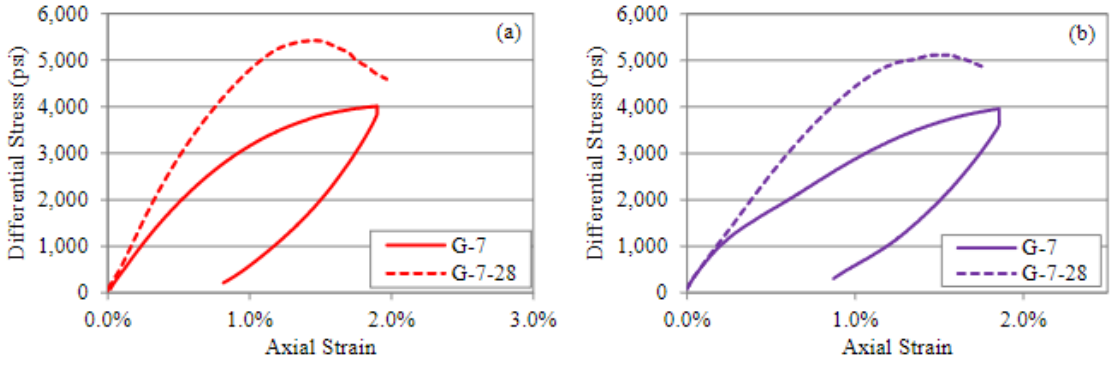

Figure 2.8: Geopolymer (G) self-healing under 3.45 MPa (500 psi) confining pressure for samples (a) and (b). Initial loading beyond the yield point of the sample occurred at 7 days, and retesting to failure occurred at 28 days. Reprinted with permission from [11].

In a different study, a group of researchers interested in the use of geopolymers as an alternative cement investigated the magnitude of self-healing in a geopolymer mortar subjected to bending. Beam specimens were prepared using a Class F fly ash and a mixture of sodium hydroxide and sodium silicate. The specimens were initially cured and loaded in a three-point bending test to a predetermined crack mouth opening (CMOD), then were allowed to heal for 14, 28 and 56 days before being retested in flexure to failure [26]. The results illustrated in Figure 2.9 denote a clear increase in tensile strength for all beam specimens regardless of age. However, the results also showed that as the geopolymers aged, their self-healing ability decreased, likely due to the extent of the geopolymerization reaction nearing completion. Even though this decreasing relationship is present, the percentage increase in strength for all the samples was still positive, showing good self-healing ability with respect to tensile strength recovery. Further microstructural analysis of healing products formed would benefit the discussion of self-healing in alkali-activated materials, since little is known about the self-healing products formed, especially in low-calcium systems.

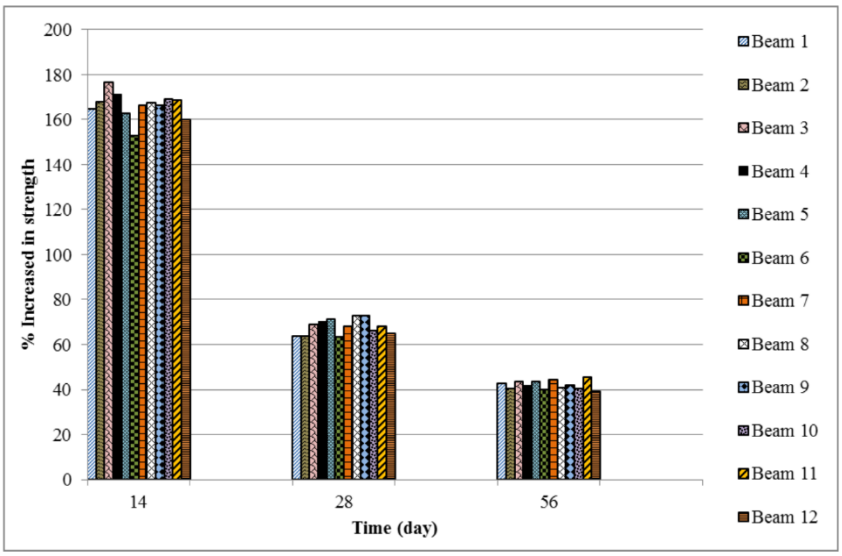

Figure 2.9: Percentage increase in tensile strength for geopolymer mortar beams at different ages. Reprinted with permission from [26].

An investigation into the self-healing ability of alkali-activated fiber-reinforced slag composites at early ages tested the effects of activators with mixtures reinforced by polyethylene fibers [40]. Activators included calcium hydroxide, sodium hydroxide, and sodium silicate. Samples were pre-loaded past their initial yield point using a uniaxial tensile test at 7 days and were later tested to failure after a healing period of 36 days. The results from the tensile tests, one sample shown in Figure 2.10, convey the greater stiffness the material had after self-healing. Analyzing the microstructure of these composites, various calcium-based phases such as calcium-(sodium) aluminosilicate hydrate (C-(N)-A-S-H) and C-S-H formed. This is likely because slag has a significantly higher calcium content than Class F fly ashes. Researchers concluded from EDXS results that C-(N)-A-S-H was the dominant healing material and suggested this was the result due to a low amount of sodium ions present in the solution along with a pH around 10 [40]. The C-(N)-A-S-H and C-A-S-H gel products that formed as part of the self-healing process could be

compared to the continued hydration process seen in portland cement systems with the formation of C-S-H. In this case, the unreacted slag particles exposed in the cracks encountered activator and created gel phases depending on the pH [40]. More work is certainly needed to identify healing products present in AAMs and comparisons need to be made to portland cement systems, as there is little known beyond the regain of mechanical properties.

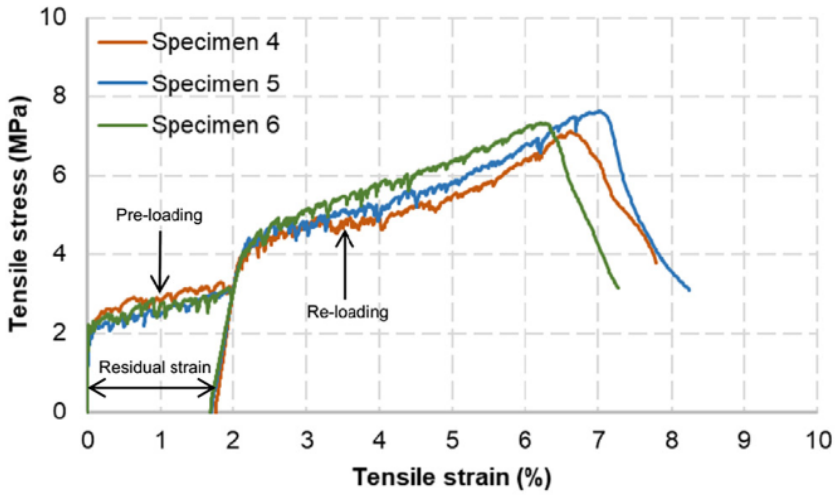

Figure 2.10: Tensile self-healing behavior in a sodium silicate activated slag composite. Reprinted with permission from [40].

Chapter 3: Materials and Methods

This chapter provides a brief description of the materials and testing methods. Section 3.1 identifies materials used in this study while Section 3.2 describes experimental methods used to evaluate permeability, tensile strength, and compressive strength.

3.1 MATERIALS

3.1.1 Fly ash

Fly ash used in this study was obtained from Newberg, MD, USA. The chemical composition of the fly ash, analyzed by x-ray fluorescence, is shown in Table 3.1.

3.1.2 Portland cement

The portland cement used in experiments was Class H obtained from Texas Lehigh Buda Plant (October 2019). The data from the mill sheet for the cement are included in Table 3.1. All cement slurries were prepared with a water-to-cement ratio by mass (w/c) of 0.385.

Table 3.1 : Oxide Composition for Class F fly ash and Class H portland cement used in this study

Component	Weight %	Weight %
	Class F fly ash	Class H OPC
SiO_2	46.45	18.2
Al_2O_3	24.09	3.9
Fe_2O_3	20.05	6.9
$SiO_2+Al_2O_3+Fe_2O_3$	90.59	29
CaO	3.08	61.7

MgO	0.79	1.0
Alkalis (Na_2O +0.658K_2O)	1.88	0.73
SO_3	0.52	3.0
TiO_2	1.15	N/A
LOI (750°C)	0.82	1.2

3.1.3 Alkaline solutions

All alkaline solutions used in this study were 8M sodium hydroxide. The solutions were prepared by dissolving reagent grade sodium hydroxide pellets in ultra-pure water (resistivity 18MΩ-cm). Alkaline solutions were cooled to room temperature prior to mixing. Based on previous work by Liu [3], the water to solids ratio (w/s) was set to 0.33, since this mixture met both the fresh state and mechanical properties ideal for well cements. The alkalis present in the alkali solution were converted to an equivalent Na_2O content and included along with the fly ash in the calculation of the solids for the mixture. The activator solution-to-fly ash mass ratio was held at 0.485 to keep the molarity of the alkaline solution at 8M.

3.2 METHODS

The methods for mixing the fly ash, alkaline solution, and cement slurries are described in this section along with relevant test methods.

3.2.1 Mixing and Curing Procedures

Cement slurries were prepared following API standard RP 10B-2 (2010). Geopolymer slurries were prepared by hand-mixing the fly ash into the alkaline solution to

a uniform consistency and then using drill mixer with a paddle stirrer at 850 rpm for 35 seconds. All curing was at atmospheric pressure in a 76.7°C (170°F) general purpose water bath.

3.2.2 Thermal Shock Procedure

A thermal shock procedure was developed with inspiration from ASTM C666 and from a DOE study of geothermal cements [41]. ASTM C666 [42], involves the repeated cycling of concrete samples from 40°F to 0°F to determine the effects of freezing and thawing on the properties of concrete. Equation (3.1) denotes the stress that the material undergoes based on a temperature change:

$$\sigma = E\alpha\Delta T \quad (3.1)$$

where σ = thermal stress, E = modulus of elasticity, α = coefficient of thermal expansion, and ΔT = change in temperature. If the thermal stress is greater than the strength of the material, damage in the form of cracking will occur.

The coefficient of thermal expansion is not currently known for geopolymers, so a large temperature differential was used to maximize thermal stresses. Removing the samples from a water bath at 76.7°C (170°F), samples were immersed in liquid nitrogen at a temperature on the order of -196°C (-320°F). Geopolymer samples were immersed in liquid nitrogen for 30 seconds, room temperature for 1 minute, and then placed back into a 76.7°C (170°F) water bath for 5 minutes. This cycle was repeated 3 times to create thorough micro-cracking.

3.2.3 Compressive Strength

The unconfined compressive strength (UCS) was determined following ASTM C39 [43]. Cylinders 25 mm (2 in.) in diameter and 50 mm (4 in.) in height were loading in

compression until failure. Neoprene pads were used during all tests to reduce point loading effects.

3.2.4 Self-Healing Testing using Unconfined Compressive Strength Measurement

The first self-healing tests performed followed the procedure developed by Liu [3], where cylinders are pre-loaded after 7 or 28 days of curing to 30%, 50%, and 70% of their average 7 or 28-day UCS, respectively. After preloading, the samples were placed back into the water bath at 76.7°C (170°F), in a 2M sodium hydroxide solution. Besides preventing leaching of the alkalis from the geopolymer, the 2M sodium hydroxide solution is representative of a typical conditioning solution used in autogenous self-healing studies to simulate the presence of an alkali pore solution. The samples preloaded after 7 days were left in the 76.7°C (170°F) bath for 21 additional days, before being retested to failure at 28 days. The percent strength relative to non-preloaded samples at 28 days was calculated and used as a metric for autogenous self-healing. The same metric was used for tests conducted with preloading at 28 days, healing for an additional 28 days, and testing to failure at 56 days of age.

3.2.5 Tensile Strength

Tensile strength for cylinders was determined using a modified version of the ASTM C496 standard [44] to account for a smaller sample size. Strengths were calculated using equation 3.2:

$$T = \frac{2P}{\pi LD} \quad (3.2)$$

where T = tensile strength (psi), P = load (lbs.), L = length of specimen (in.), and D = diameter of specimen (in.). Samples were cured in a 76.7°C (170°F) for 14 days prior to testing. The average strength was calculated based on the average of 3 replicate samples.

3.2.6 Pressure Transmission Testing

Pressure transmission testing (PTT) was included to obtain novel values of permeability for geopolymer samples and investigate the autogenous self-healing of the geopolymer microstructure. PTT was introduced to the oil/gas industry by van Oort [28], who showed how pressure transmission could be used with drilling fluids to investigate pore-pressure effects in shales. In this technique, a sample is inserted into an elastomer sleeve and placed into a vessel where a confining pressure constricts the sleeve around the sample. A full system diagram is outlined in Figure 3.1. Before testing, the sample is fully saturated by applying pressure to a pore solution on both sides of the sample and waiting for equilibrium to be reached for temperature and pressure. At the start of the test, a downstream reservoir is created by means of a cutoff valve, which cuts off the downstream reservoir from the upstream reservoir. Overbalance pressure is applied by increasing the upstream pressure. The pressure diffusion through the sample is recorded on the downstream side as the sample transmits the fluid due to the difference in pressure, allowing for the calculation of the permeability of the sample through the manipulation of equation (3.3) to equation (3.4) to solve for permeability [28]:

$$\frac{\mathrm{P(l,t)} - \mathrm{P_0}}{\mathrm{P_m} - \mathrm{P_0}} = 1 - \exp\left[-\frac{\mathrm{Akt}}{\mu\beta\mathrm{Vl}}\right] \quad (3.3)$$

$$\mathrm{k} = \frac{\mu\beta\mathrm{Vl}}{\mathrm{A}} \frac{\Delta\ln\left(\frac{\mathrm{P_m} - \mathrm{P_0}}{\mathrm{P_m} - \mathrm{P(l,t)}}\right)}{\Delta\mathrm{t}} \quad (3.4)$$

where P_0 = initial pore pressure (Pa), P_m = upstream fluid pressure (Pa), $P(l,t)$ = downstream fluid pressure (Pa), l = length (m), t = time (s), k = permeability (D), A = area

(m^2), V = downstream reservoir volume (m^3), μ = fluid viscosity ($Pa \cdot s$), t = time (s), and β = fluid compressibility (Pa^{-1}).

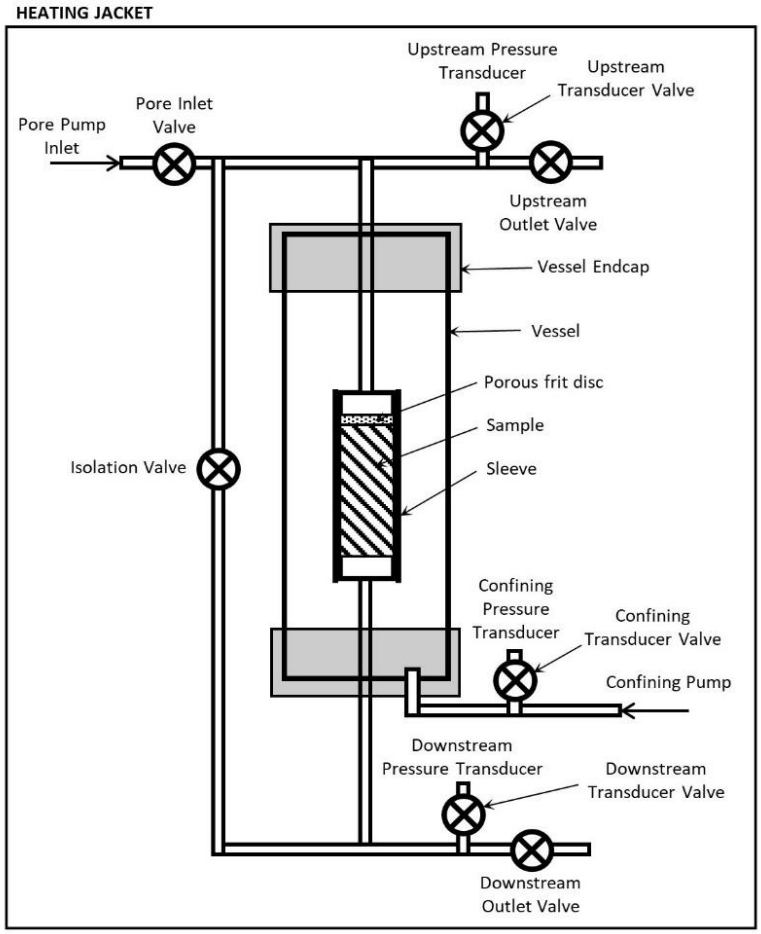

Figure 3.1: Schematic of the PTT system.

In the first study dedicated to determining fluid permeability values for geopolymers, samples were cast into 76mm (3 in.) diameter PVC molds and cured following the standard curing procedure. The samples were subsequently cored and cut to 50 mm (2 in.) length and 25 mm (1 in.) diameter samples before being tested, always

ensuring that the samples remained saturated with a weak alkali solution to minimize leaching of alkalis. Three replicate samples were tested at 7, 14, and 28 days to determine an average permeability value. As shown in Figure 3.1, porous aluminum frits were placed between the top of the sample and the head, directing uniform flow across the sample. The stack was placed into a heat shrink tubing sleeve and wrapped with tie wire to seal the system. Heat was applied to constrict the tubing around the stack before it was placed inside the vessel and heating jacket, set to 40°C (104°F). Two syringe pumps were filled with tap water, which served as the pore fluid for each test. A confining pressure of 2.06 MPa (300 psi) was applied, creating a radial confining stress around the sample. Initial pore pressure of 0.138 MPa (20 psi) was set to saturate the geopolymer samples before each test was run. To begin the test, the downstream was isolated by means of a valve, and the pore pressure in the upstream was ramped to 0.483 MPa (70 psi). Values from literature for the compressibility [45] and viscosity of water [46] were used in the calculation of the permeability (k).

3.2.7 Steady State N_2 Gas Permeability

Metarock laboratories conducted steady state gas permeability testing using a Metarock Ultra Low Perm gas permeameter. The system measured the stressed state permeability over time at an effective stress of 6.90 MPa (1000 psi) and a temperature of 40°C (104°F). Nitrogen gas was used in the test because the ability of the software system to correct for the Klinkenberg gas slippage effect. Results reported are the absolute gas permeability of the samples.

3.2.8 Self-Healing Permeability Test

Self-healing permeability tests followed a similar procedure to that described in Section 3.2.4, except thermal shock was used to damage the samples rather than compression loading. The permeability of virgin 7-day old samples was determined using the pressure transmission test before thermal shocking as described in Section 3.2.2. After being thermally shocked, the samples were retested using the pressure transmission method to determine the sample permeability after damage. The samples were then allowed to heal in a 2M NaOH conditioning solution for 21 additional days. The samples were retested using the pressure transmission method for a final permeability at 28-days to determine a degree of permeability recovery.

Chapter 4: Results and Discussion

4.1 Strength Evolution of Geopolymer Pastes

As previously presented, geopolymer properties vary depending on the activator, binder, and other variables [3]. To establish a baseline for self-healing tests where UCS was used, a UCS study was conducted on the geopolymer mixture through 56 days to establish early and late strengths. UCS measurements were taken at 1, 3, 7, 21, 28, and 56 days. The results are shown in Figure 4.1. The error bars on all plots represent the minimum and maximum strengths from 3 replicate samples.

Oil well cements are not typically tested through a period of 56 days, but rather they are tested for the time it takes to reach a 3.45MPa (500 psi) strength, the minimum required before restarting drilling operations. Since the cement sheath is subject to stresses beyond early ages [1], it is important to look at strength gains outside of this initial strength development period. Within error, the strength gain for this mixture primarily occurred within the first 7 days of age. At 1 day of age, the mixture already exceeded the 3.45 MPa (500 psi) minimum strength. By 28 days, the standard length of time for structural concrete UCS testing, the mixture had a minimum strength of 27.6 MPa (4000 psi), which is well within the range of strengths used in structural concrete [47]. This result also correlates well with the strengths Liu and Liu et al. [3], [11] reported for the mixture used in unconfined self-healing tests.

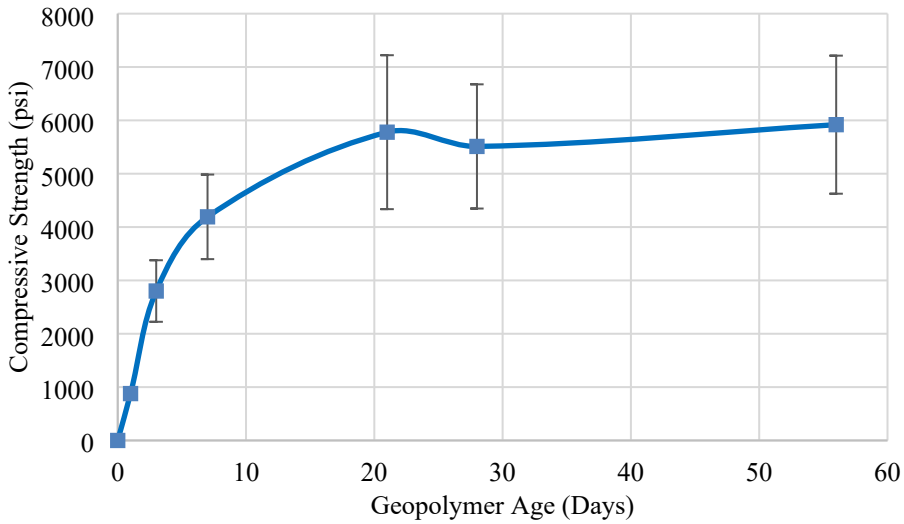

Figure 4.1: Strength evolution for w/s 0.33 geopolymer paste.

4.2 Confirmation of Unconfined Self-Healing Behavior

To confirm results previously obtained by Liu [3], geopolymer and cement paste samples were tested for unconfined compressive strength after self-healing as described in Section 3.2.4. This procedure follows the exact procedure Liu [3] described, where cylinders were pre-loaded after 7 or 28 days of curing to 30%, 50%, and 70% of their average 7 or 28-day UCS, respectively. The 7-day samples were cured for an additional 21 days before being retested in compression to failure, and the 28-day samples were cured for an additional 28 days before failure. The results from this testing are shown in Figure 4.2. The horizontal axis shows the pre-loading level at 7 or 28 days, while the vertical axis denotes the compressive strength relative to the 28 or 56-day average compressive strength of non-preloaded samples. The error bars and regions on all plots represent the minimum and maximum strengths from 3 replicate samples.

In order to demonstrate self-healing, the average compressive strength of the cracked samples should be at least as strong as the virgin uncracked samples. Figures 4.2 and 4.3 convey that all samples had strengths that within error are 100% equivalent to virgin samples. Thus, self-healing may have occurred, but the averages do not support this conclusion within the observed range of experimental error, unfortunately. Overall, the variability in the UCS results is simply too great to make a conclusion one way or another. Expectations of self-healing for unconfined compression preloading of geopolymers were set high based on the work by Liu and Liu et al. [3], [11], who showed that all geopolymers samples not only exceeded the 100% baseline strength of virgin samples after 21 or 28 days of healing, but clearly outperformed portland cement samples which decreased in strength. An error bar for the virgin samples which establish the red 100% strength baseline on plots were missing in results Liu and Liu et al. reported [3], [11]. Therefore, it is difficult to determine how much variability the 100% baseline may have had, and if it overlapped with healed strengths. It should be noted, however, that our results here are not in disagreement with those of Liu and Liu et al.

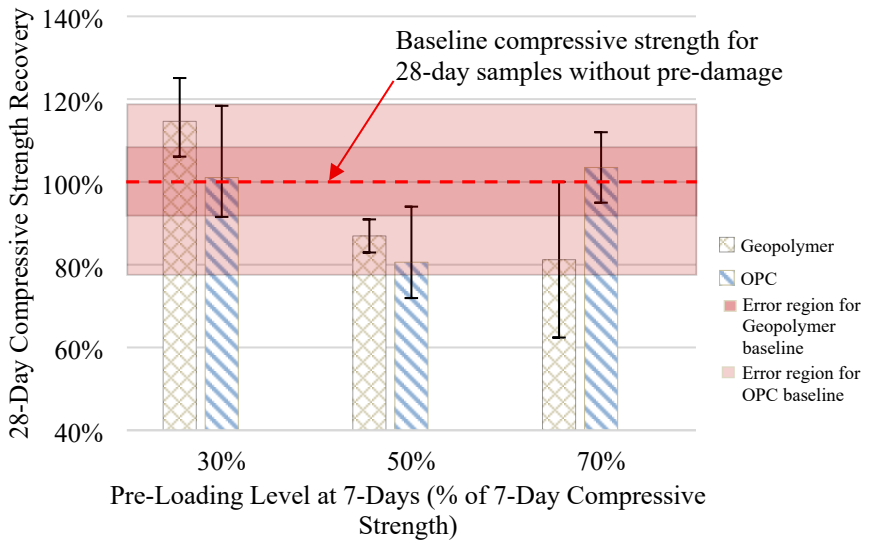

Figure 4.2: Compressive strength recovery of portland cement and geopolymer samples pre-loaded at 7 days and retested to failure at 28 days.

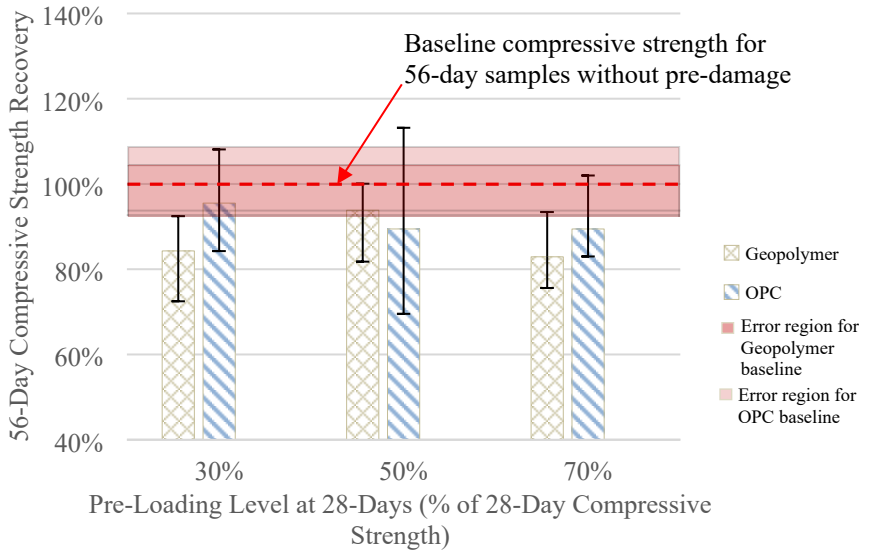

Figure 4.3: Compressive strength recovery of portland cement and geopolymer samples pre-loaded at 28 days and retested to failure at 56 days.

4.3 Effect of Thermal Shock on Tensile Strength

Based on the successful use of three-point bending in the investigation of autogenous self-healing in geopolymer mortars [26], a splitting tensile test setup was created to investigate the tensile strength recovery of geopolymers after cracking and self-healing. Samples were cured in a 76.7°C (170°F) for 14 days prior to testing. After establishing a baseline of tensile strength for geopolymers and portland cement, samples were immersed in nitrogen following the freeze-thaw procedure described in Section 3.2.2 to determine the effect of thermal shock on tensile strength. Error bars in Figure 4.4 denote the minimum and maximum tensile strengths recorded for each set of tests.

As shown in Figure 4.4, within error, up to three freeze-thaw cycles had no effect on the tensile strength of the samples. To further investigate why the freeze-thaw cycles had no effect, a geopolymer sample was freeze-thaw tested until failure. The crack plane, shown in Figure 4.5, clearly shows large radial crack propagation, but not through the center of the sample. The nitrogen caused micro-cracking on the outside of the samples, but the large sample size prevented the cracks to extend throughout the sample. Thus, a smaller diameter sample size, to be used in the pressure transmission test, was chosen to investigate self-healing through permeability testing.

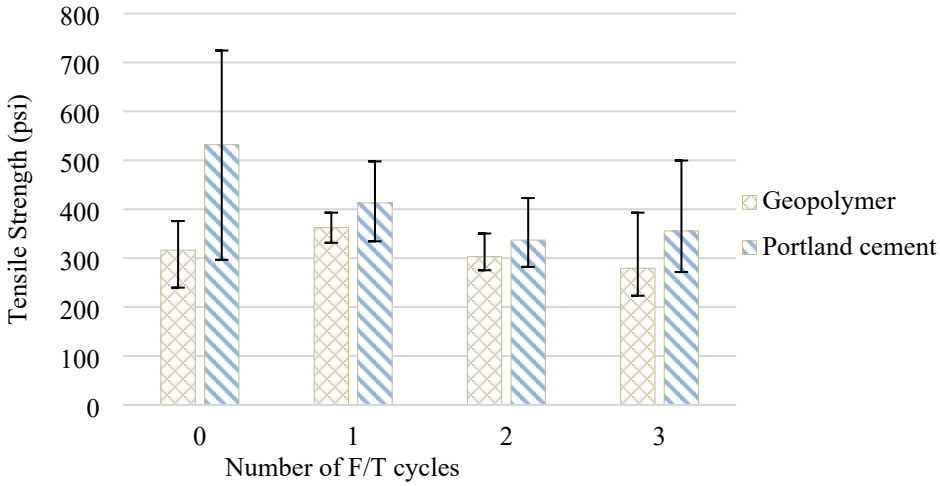

Figure 4.4: Tensile strength versus freeze-thaw cycles for geopolymer and portland cement samples at 14 days.

Figure 4.5: Crack plane of a geopolymer sample freeze-thaw tested to failure at 14 days.

4.4 PERMEABILITY OF GEOPOLYMERS

Pressure transmission curves for three samples at 7, 14, and 28 days are shown in Figures 4.6, 4.7, and 4.8. Results showed good permeability across all three samples. The permeability averaged 4.47μD at 7 days, 0.293μD at 14 days, and 0.260μD at 28 days. These are novel values for fly ash-based geopolymers and have not been previously reported in literature. The permeability evolution with time is shown in Figure 4.9, denoting a clear decrease in permeability as the microstructure of the geopolymer develops. Error bars denote the minimum and maximum permeability values recorded for each set of tests. The permeability levels off around 14 days, indicating that the geopolymerization reaction has neared completion at this point. Comparing the permeability of geopolymers to portland cement slurries, it is well below the recommended 100μD recommended by API [35] for oil well cements, and well within the range of permeabilities for Class H and G portland cement slurries [32], [48].

To ensure accuracy of results, external and independent pressure transmission testing by Metarock Laboratories was commissioned for 3 additional replicate geopolymer samples at 14 days of age. Metarock reported an average permeability of 0.723μD, shown in Figure 4.10, illustrating consistency compared to results shown in Figure 4.7. Some permeability variation is expected given that the samples are from a different mixture. Steady state N_2 gas permeability tests were also run on all three geopolymer samples, shown in Figures 4.11, 4.12, and 4.13. The effective confining stress for all tests was 6.90 MPa (1000 psi). The average gas permeability of the geopolymer samples was 21.8μD.

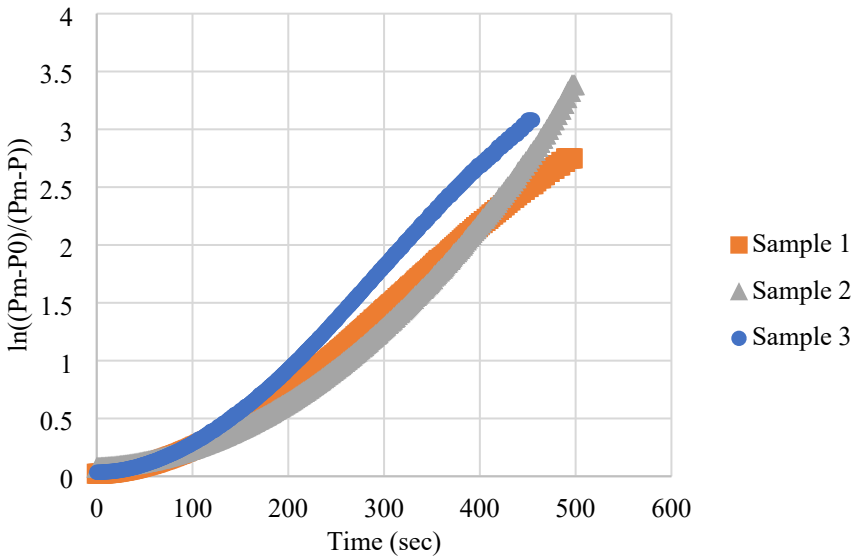

Figure 4.6: Repeatability of pressure build-up curves for three replicate geopolymer samples at 7 days of age.

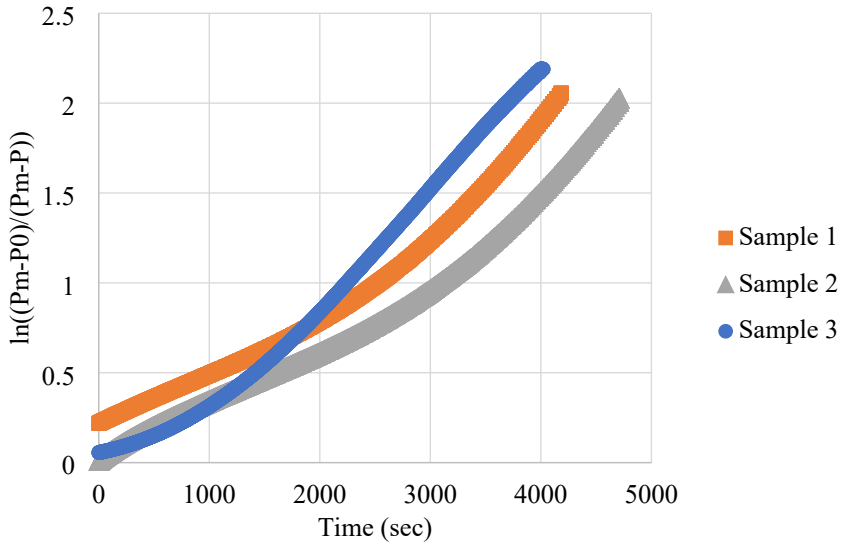

Figure 4.7: Repeatability of pressure build-up curves for three replicate geopolymer samples at 14 days of age.

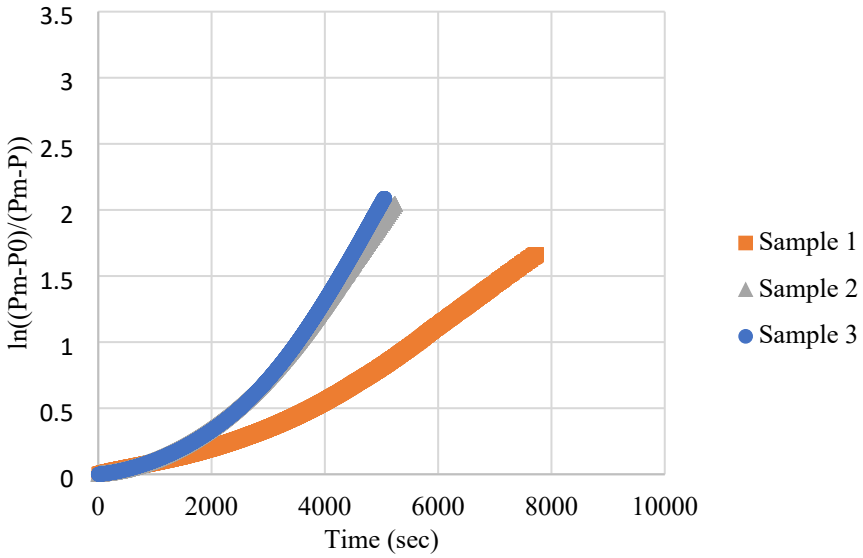

Figure 4.8: Repeatability of pressure build-up curves for three replicate geopolymer samples at 28 days of age.

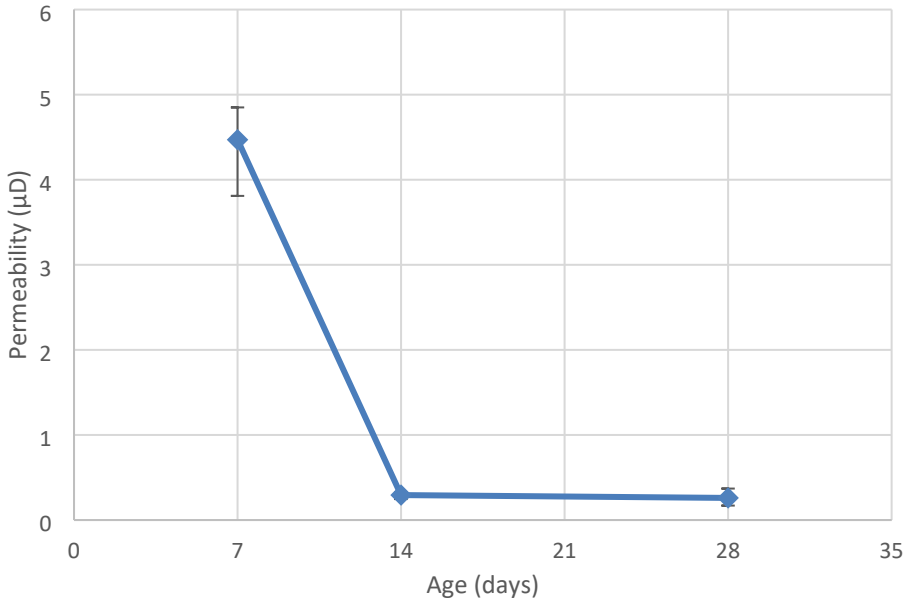

Figure 4.9: Permeability evolution of geopolymers.

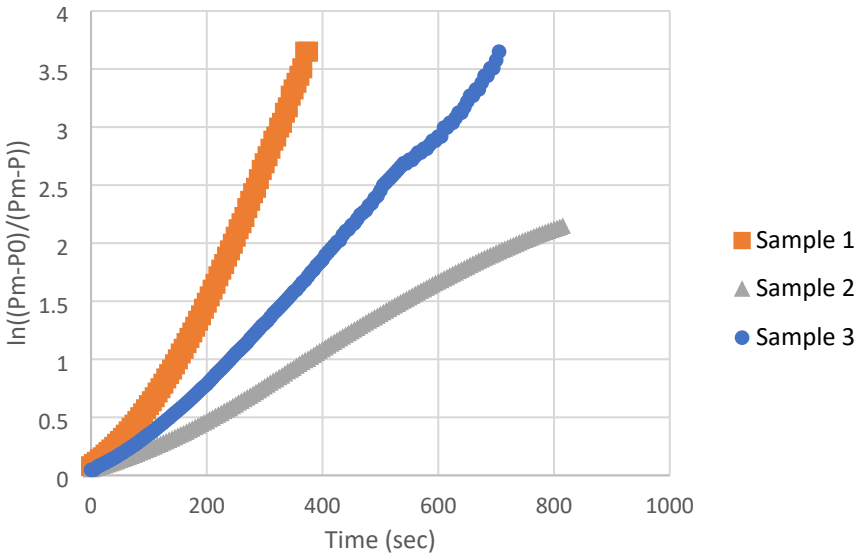

Figure 4.10: Pressure build-up curves for three replicate geopolymer samples at 14 days of age. Testing was done by Metarock Laboratories.

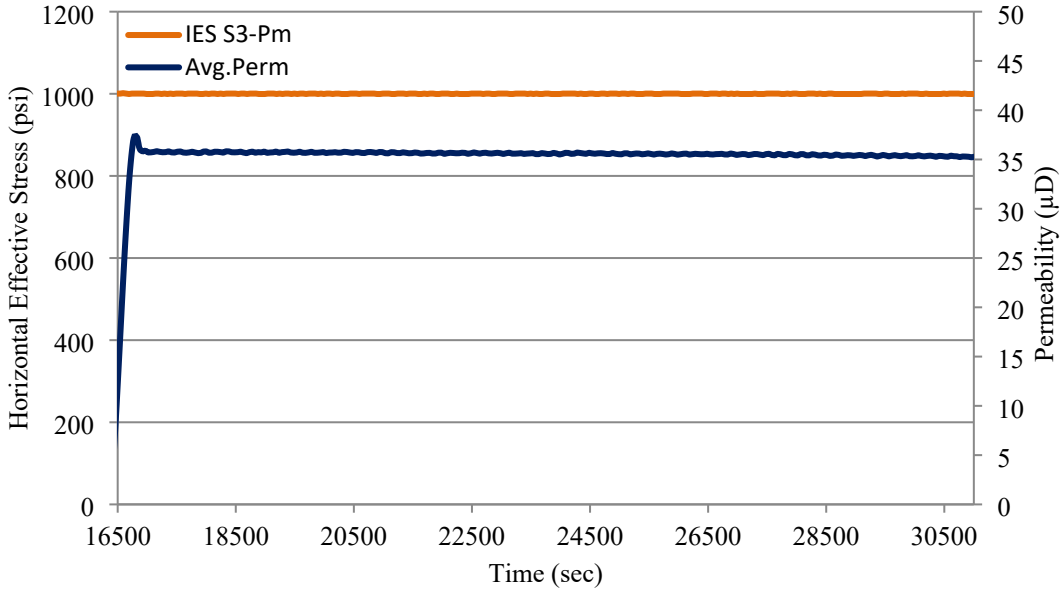

Figure 4.11: Steady state N_2 gas permeability at 6.90 MPa (1000 psi) effective stress for geopolymer sample 1. Testing done by Metarock Laboratories.

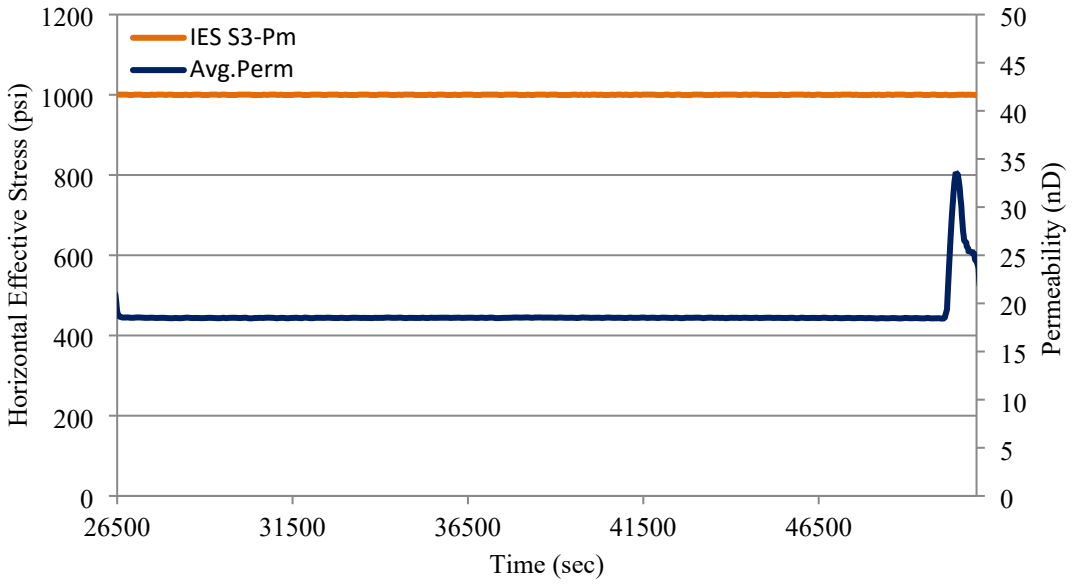

Figure 4.12: Steady state N_2 gas permeability at 6.90 MPa (1000 psi) effective stress for geopolymer sample 2. Testing done by Metarock Laboratories.

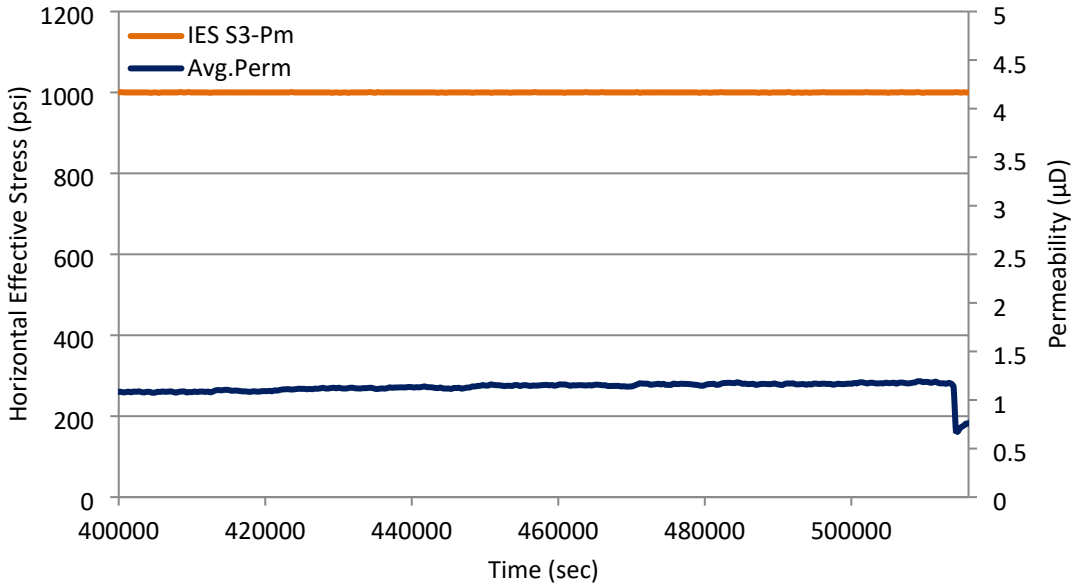

Figure 4.13: Steady state N_2 gas permeability at 6.90 MPa (1000 psi) effective stress for geopolymer sample 3. Testing done by Metarock Laboratories.

4.5 Micro-cracking Confirmation using Micro Computed Tomography

Initial trials of micro-cracking used a 50 mm (2 in.) diameter cylinder, but thermal shock tests showed that micro-cracking did not propagate through the core of the sample (Figure 4.5). To ensure that the thermal shock procedure was creating thorough micro-cracking in the 25 mm (1 in.) sample size, a portland cement sample was thermally shocked after 14 days of curing and scanned using μCT. Two slices from the scans are shown in Figure 4.14, showing a clear variety of shape and size in the micro-cracks. This confirmed that the process to use the thermal shock procedure described in Section 3.2.2 with 25 mm (1 in.) cores successfully created micro-cracks and could be used to investigate the self-healing of cement and geopolymer slurries through permeability measurements.

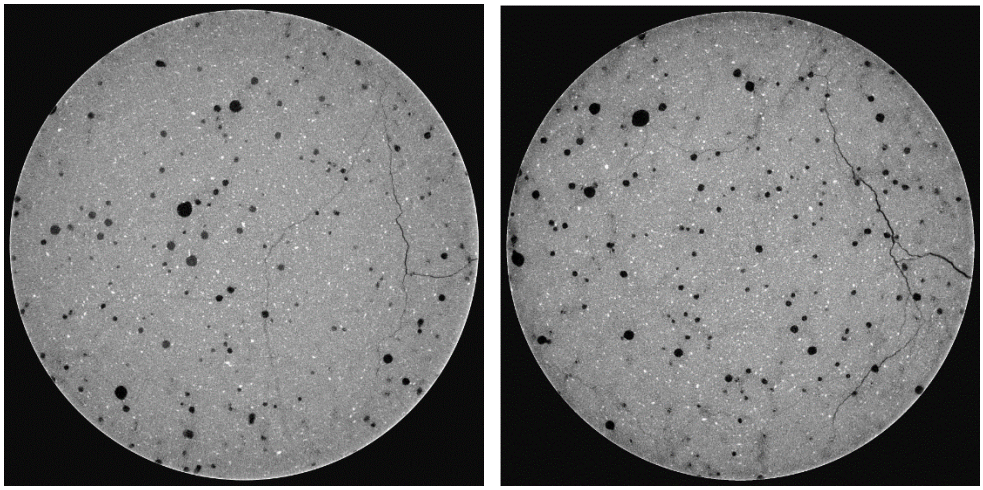

Figure 4.14: μCT images for a thermally shocked portland cement sample.

4.6 Using Permeability to Detect Self-Healing

With a successful method to micro-crack samples, three geopolymer samples were thermally shocked after 7 days of curing and allowed to heal in a 2M NaOH conditioning solution for 21 days. The results from the pressure transmission tests that tested the self-

healing at initial, damaged, and healed states of geopolymers are shown in Figures 4.15, 4.16, and 4.17, ordered with increasing initial damage caused by thermal shock using liquid nitrogen (LN_2). Pre-LN_2 refers to the 7-day virgin permeability, while post-LN_2 refers to the permeability after thermal shock. Each sample was exposed the same number of freeze-thaw cycles, but due to the random nature of micro-cracking, a different degree of initial damage occurred in each of the samples. There is an increase in permeability across all three samples after the thermal shock (blue line compared to orange line). Moreover, all samples show permeability recovery after self-healing (orange line to gray line).

Results for sample 1, the least damaged sample, shown in Figure 4.15, indicate the greatest degree of self-healing, with the healed permeability being lower than the initial permeability at 7 days. Thermal shock damage nearly doubled the permeability of the sample from 4.09μD to 9.48μD, but the permeability then decreased to 2.76μD after healing, showing great ability to self-heal. On the other hand, sample 3 was the most damaged sample, with a decrease in permeability from 25.8μD to 16.23μD as shown in Figure 4.17. This sample was so extensively damaged that it was not capable of fully recovering its initial, low permeability. However, it still exhibited healing, decreasing the permeability to 16.23μD after the healing time. Sample 2, with an intermediate degree of initial cracking, showed that a medium amount of damage correlates with a medium amount of self-healing, as illustrated in Figure 4.16. Comparing with virgin samples of the same age, samples after self-healing did not approach the 0.26μD average permeability. This indicates that damage to the micro-structure can be self-healed to a degree, but some damage apparently remains irreparable and irrecoverable, at least under the conditions of our re-healing tests.

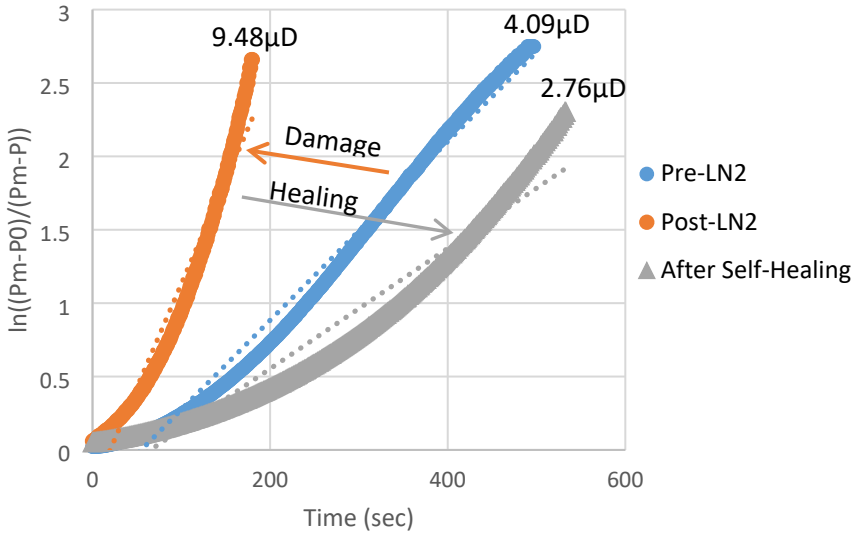

Figure 4.15: Permeability damage and recovery from LN_2 thermal shock for geopolymer sample 1.

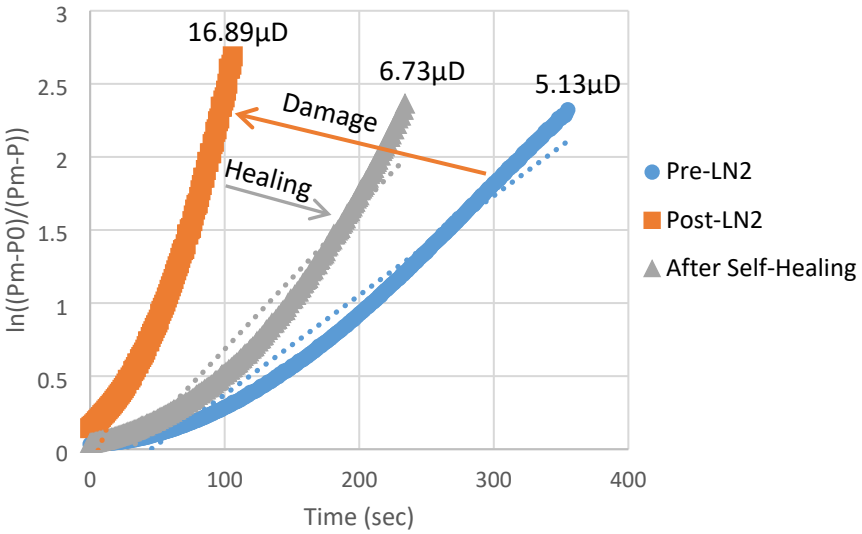

Figure 4.16: Permeability damage and recovery from LN_2 thermal shock for geopolymer sample 2.

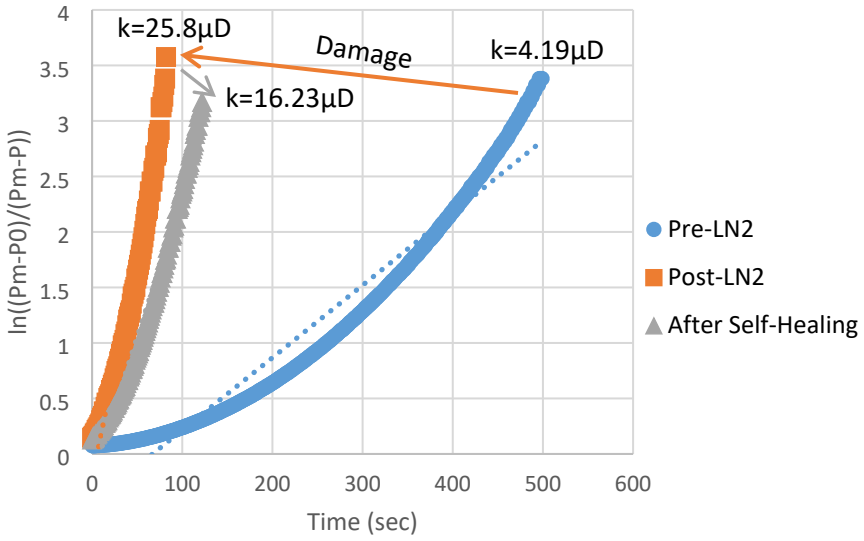

Figure 4.17: Permeability damage and recovery from LN_2 thermal shock for geopolymer sample 3.

Chapter 5: Conclusions and Suggestions for Future Work

5.1 CONCLUSIONS

In this study, the self-healing ability of fly ash based geopolymers was investigated. The main findings are:

- Unconfined compressive strength testing showed that low calcium fly ash-based geopolymers activated using an 8M NaOH solution and cured at 76.7°C (170°F) easily outperform oil well cementing strength requirements and also fall within the strength requirements of structural concretes. Within error, most of the strength gain occurred within the first 7 days.
- Unconfined compressive strength testing, however, was not sensitive enough to accurately assess if self-healing was occurring in the samples tested.
- Splitting tensile strength testing is not reliable to assess self-healing with thermal shock damage. The thermal shock induces random micro-cracks that propagate from the outside edge of the cylinders inward towards the center, but splitting tensile strength testing tests a single fracture plane where it is unlikely to test the damaged areas consistently.
- A thermal shock procedure developed for this research caused micro-cracking in 50 mm (2 in.) diameter geopolymer samples, but cracking did not propagate through the center core of samples, as confirmed by visual examination of sample cross-section.
- The same thermal shock procedure on a 25 mm (1 in.) diameter core resulted in a more dispersed and homogenous micro-crack distribution with cracks propagating through the core of a sample, as confirmed by μCT scans.

- Permeability testing of geopolymers at 7, 14, and 28 days showed a decrease in permeability over time as the microstructure developed, leveling off around 0.26μD. This value is low enough to maintain hydraulic isolation in a wellbore environment and prevent hydrocarbon migration at any detectable rate.
- The thermal shocking procedure was used on small cores, 25 mm (1 in.) diameter, to assess self-healing of geopolymer samples through permeability testing. Regardless of initial damage, each sample self-healed and reduced in permeability after thermal shock and saturation in a conditioning solution for 21 additional days. A smaller initial damage to samples resulted in a greater degree of self-healing, while samples that had extensive initial damage showed a reduced ability to self-heal. Compared with virgin samples at the same age, samples after self-healing did not approach the 0.26μD average permeability, suggesting that while geopolymers are capable of self-healing, initial damage to the samples results in some irreparable damage under the conditions of the tests reported here.

5.2 Suggestions for Future Work

- The permeability evolution over time for a single geopolymer mixture was shown in this study, but the same setup can be expanded to other cementitious or geopolymer samples to further compare and optimize mixtures for wellbore applications.
- Given the promising initial results presented on the self-healing of geopolymers through permeability measurements, this method of self-healing evaluation could be expanded to other mixtures and systems such as potassium hydroxide-activated

geopolymers, silicate-activated geopolymers, or geopolymers made from other fly ash sources.

- The thermal shock procedure used resulted in a varied and extensive damage to the sample, as demonstrated by permeability measurements. Reducing the number of freeze-thaw cycles down from 3 may result in a more consistent and reduced damage of the sample. The temperature range used to thermally shock the sample could also be reduced by cooling the samples down to room temperature (from their curing/self-healing bath temperature of 76.7°C (170°F)) before exposing them to LN_2. This would reduce the degree of damage as well. Determining the thermal expansion coefficient for geopolymers could also be of use in this area, as the thermal stresses induced in the samples could subsequently be calculated.
- μCT scans were employed in this study solely to visually confirm micro-cracking in a sample, but scans could be quantitatively processed to determine crack closure volume. An initial scan of a sample would give a baseline volume of cracks in the sample (presumably zero), while a scan after damage would allow for the determination of the induced crack volume. A final scan could occur after the healing period to determine crack closure by comparing initial and final crack volumes.

Bibliography

[1] E. van Oort, M. Juenger, X. Liu, and M. McDonald, "Silicate-activated geopolymer alternatives to Portland cement for thermal well integrity," in *Society of Petroleum Engineers - SPE Thermal Well Integrity and Design Symposium 2019, TWID 2019*, 2019.

[2] T. Vrålstad, A. Saasen, E. Fjær, T. Øia, J. D. Ytrehus, and M. Khalifeh, "Plug & abandonment of offshore wells: Ensuring long-term well integrity and cost-efficiency," *Journal of Petroleum Science and Engineering*, vol. 173. Elsevier B.V., pp. 478–491, 01-Feb-2019.

[3] Xiangyu Liu, "Mud-to-Cement Conversion of Synthetic-Based Drilling Muds using Geopolymers," Ph.D Dissertation, College of Eng., Univ. of Texas at Austin, Austin, TX, USA, 2017.

[4] E. Lindeberg, P. Bergmo, M. Torsæter, and A. A. Grimstad, "Aliso Canyon Leakage as an Analogue for Worst Case CO2 Leakage and Quantification of Acceptable Storage Loss," in *Energy Procedia*, 2017, vol. 114, pp. 4279–4286.

[5] K. R. Backe, O. B. Lile, S. K. Lyomov, H. Elvebakk, and P. Skalle, "Characterizing curing-cement slurries by permeability, tensile strength, and shrinkage," *SPE Drilling and Completion*, vol. 14, no. 3, pp. 162–167, 1999.

[6] M. de Rooij, van T. Kim, N. de Belie, and E. Schlangen, *Self-Healing Phenomena in Cement-Based Materials: : State-of-the-Art Report of RILEM Technical Committee 221-SHC: Self-Healing Phenomena in Cement-Based Materials*. Springer Netherlands, 2013.

[7] L. Kan, J. Lv, B. Duan, and M. Wu, "Self-healing of Engineered Geopolymer Composites prepared by fly ash and metakaolin," *Cement and Concrete Research*, vol. 125, p. 105895, Nov. 2019.

[8] J. L. Provis and J. S. J. van Deventer, *Alkali-Activated Materials: State-of-the-Art Report, RILEM TC 224-AAM.* Springer Netherlands, 2014.

[9] J. Davidovits, "Properties of Geopolymer Cements," *First International Conference on Alkaline Cements and Concretes*, pp. 131–149, 1994.

[10] Z. Sun and A. Vollpracht, "One year geopolymerisation of sodium silicate activated fly ash and metakaolin geopolymers," *Cement and Concrete Composites*, vol. 95, pp. 98–110, Jan. 2019.

[11] X. Liu, M. J. Ramos, S. D. Nair, H. Lee, D. Nicolas Espinoza, and E. van Oort, "True self-healing geopolymer cements for improved zonal isolation and well abandonment," in *SPE/IADC Drilling Conference, Proceedings*, 2017, vol. 2017-March, pp. 130–141.

[12] J. Davidovits, *Geopolymer Chemistry and Applications*, vol. 171. 2008.

[13] I. Garcia-Lodeiro, A. Palomo, A. Fernández-Jiménez, and D. E. MacPhee, "Compatibility studies between N-A-S-H and C-A-S-H gels. Study in the ternary diagram Na2O-CaO-Al2O3-SiO2-H2O," *Cement and Concrete Research*, vol. 41, no. 9. Elsevier Ltd, pp. 923–931, 2011.

[14] A. M. M. al Bakri, H. Kamarudin, O. A. K. A. Karem, C. M. Ruzaidi, A. R. Rafiza, and M. N. Norazian, "Optimization of alkaline activator/fly ash ratio on the compressive strength of manufacturing fly ash-based geopolymer," in *Applied Mechanics and Materials*, 2012, vol. 110–116, pp. 734–739.
[15] E. Tziviloglou, "Biogenic self-healing mortar: Material development and experimental evaluation," Ph.D Dissertation, College of Eng., TU Delft, Delft, Netherlands, 2018.
[16] S. K. Ghosh, *Self-Healing Materials: Fundamentals, Design Strategies, and Applications*. 2008.
[17] M. Rajczakowska, K. Habermehl-Cwirzen, H. Hedlund, and A. Cwirzen, "Autogenous Self-Healing: A Better Solution for Concrete," *Journal of Materials in Civil Engineering*, vol. 31, no. 9, pp. 1–19, 2019.
[18] M. Wu, B. Johannesson, and M. Geiker, "A review: Self-healing in cementitious materials and engineered cementitious composite as a self-healing material," *Construction and Building Materials*, vol. 28, no. 1. pp. 571–583, Mar-2012.
[19] M. Schneider, "The cement industry on the way to a low-carbon future," *Cement and Concrete Research*, vol. 124, no. February, p. 105792, 2019.
[20] G. Habert and C. Ouellet-Plamondon, "Recent update on the environmental impact of geopolymers," *RILEM Technical Letters*, vol. 1, p. 17, 2016.
[21] H. Jonkers and E. Schlangen, "Crack repair by concrete immobilized bacteria," *Proceedings 1st International …*, no. April, pp. 1–7, 2007.
[22] S. Fan and M. Li, "X-ray computed microtomography of threedimensional microcracks and self-healing in engineered cementitious composites," *Smart Materials and Structures*, vol. 24, no. 1, Jan. 2015.
[23] E. Marangon, R. D. Toledo Filho, and E. M. R. Fairbairn, "Self-healing of Engineered Cementitious Composites in the Natural Self-healing of Engineered Cementitious," no. January 2012, 2019.
[24] L. Ferrara, "Self-healing cement-based materials: An asset for sustainable construction industry," *IOP Conference Series: Materials Science and Engineering*, vol. 442, no. 1, 2018.
[25] S. Qian and V. C. Li, "Headed anchor/Engineered Cementitious Composites (ECC) pullout behavior," *Journal of Advanced Concrete Technology*, vol. 9, no. 3, pp. 339–351, 2011.
[26] M. Ali, R. Babecki, and A. I. Abu-Tair, "Self- healing and strength development of geopolymer concrete made with Waste by products," *International Conference on Biological, Civil and Environmental Engineering*, 2015.
[27] S. Qian, J. Zhou, M. R. de Rooij, E. Schlangen, G. Ye, and K. van Breugel, "Self-healing behavior of strain hardening cementitious composites incorporating local waste materials," *Cement and Concrete Composites*, vol. 31, no. 9, pp. 613–621, 2009.
[28] E. van Oort, "A novel technique for the investigation of drilling fluid induced borehole instability in shales," *SPEIISRM Rock Mechanics in Petroleum*

Engineering Conference held in Delft, The Netherlands, 29-31 August 1994, pp. 293–308, 1994.

[29] C. Edvardsen, "Water permeability and autogenous healing of cracks in concrete," *ACI Materials Journal*, vol. 96, no. 4, pp. 448–454, 1999.

[30] J. Wang, K. van Tittelboom, N. de Belie, and W. Verstraete, "Use of silica gel or polyurethane immobilized bacteria for self-healing concrete," *Construction and Building Materials*, vol. 26, no. 1, pp. 532–540, 2012.

[31] K. Wang, D.C. Jansen, S.P. Shah, and A.F. Karr, "Permeability study of cracked concrete," *Cement and concrete research*, vol. 27, no. 3, pp. 381–393, 1997.

[32] E. B. Nelson and Dominique. Guillot, *Well Cementing*. Schlumberger, 2006.

[33] E. B. Nelson, "Well Cementing," *Developments in Petroleum Science*, vol. 28, no. C, pp. 1-4-1–4, Jan. 1990.

[34] S. Bachu and D. B. Bennion, "Experimental assessment of brine and/or CO2 leakage through well cements at reservoir conditions," *International Journal of Greenhouse Gas Control*, vol. 3, no. 4, pp. 494–501, Jul. 2009.

[35] J. P. Nogues, B. Court, M. Dobossy, J. M. Nordbotten, and M. A. Celia, "A methodology to estimate maximum probable leakage along old wells in a geological sequestration operation," *International Journal of Greenhouse Gas Control*, vol. 7, pp. 39–47, Mar. 2012.

[36] Y. Yang, E. H. Yang, and V. C. Li, "Autogenous healing of engineered cementitious composites at early age," *Cement and Concrete Research*, vol. 41, no. 2, pp. 176–183, 2011.

[37] Y. Yang, M. D. Lepech, E. H. Yang, and V. C. Li, "Autogenous healing of engineered cementitious composites under wet-dry cycles," *Cement and Concrete Research*, vol. 39, no. 5, pp. 382–390, 2009.

[38] V. C. Li and T. Kanda, "Structural Applications of Engineered Cementitious Composites," *Journal of Materials in Civil Engineering*, 1998.

[39] M. Rajczakowska, K. Habermehl-Cwirzen, H. Hedlund, and A. Cwirzen, "The Effect of Exposure on the Autogenous Self-Healing of Ordinary Portland Cement Mortars," *Materials*, vol. 12, no. 23, p. 3926, 2019.

[40] H. H. Nguyễn, J. il Choi, H. K. Kim, and B. Y. Lee, "Effects of the type of activator on the self-healing ability of fiber-reinforced alkali-activated slag-based composites at an early age," *Construction and Building Materials*, vol. 224, pp. 980–994, 2019.

[41] T. Sugama and T. Pyatina, "Self-Healing, Re-adhering, and Corrosion-Mitigating Inorganic Cement Composites for Geothermal Wells at 270-300C," 2019.

[42] "ASTM C666-97, Standard Test Method for Resistance of Concrete to Rapid Freezing and Thawing," *ASTM International*. West Conshohocken, PA, 1997.

[43] "ASTM C39 / C39M-20, Standard Test Method for Compressive Strength of Cylindrical Concrete Specimens," *ASTM International*. West Conshohocken, PA, 2020.

[44] "ASTM C496 / C496M-17, Standard Test Method for Splitting Tensile Strength of Cylindrical Concrete Specimens," *ASTM International*. West Conshohocken, PA, 2017.
[45] R. A. Fine and F. J. Millero, "Compressibility of water as a function of temperature and pressure," *The Journal of Chemical Physics*, vol. 59, no. 10, pp. 5529–5536, Nov. 1973.
[46] L. Korson, W. Drost-Hansen, and F. J. Millero, "Viscosity of Water at Various Temperatures," *The Journal of Physical Chemistry*, vol. 73, no. 1, pp. 34–39, 1968.
[47] S. H. Kosmatka, M. L. Wilson, and P. C. Association., *Design and Control of Concrete Mixtures*. 2016.
[48] O. A. Omosebi, "Mechanical Degradation Of Well Cement In HPHT Carbonic Acid Environment: Experimental Studies And Mathematical Modeling," Ph.D dissertation, School of Petr. and Geo. Eng., Univ. of Oklahoma, Norman, OK, USA, 2016.